A note on saturation transitions between water vapor and cloud droplets

Peter A. Taylor [a]

[a] *Centre for Research in Earth and Space Science, York University, Toronto, M3J 1P3, Canada*

Corresponding author: Peter A. Taylor (pat@yorku.ca)

1 Jan 2024

ABSTRACT

In warm clouds and fog there are transitions between water vapor and cloud droplets. Within an air parcel these saturation adjustments can often be assumed to occur rapidly relative to other processes and we can use a simple mass and heat conserving transition to determine the change in temperature, and mixing ratios for water vapor and liquid water in the parcel. This note describes and tests a simple one-moment BMP (Bulk Microphysical Parameterization) procedure that we use in fog and stratus cloud modelling situations in order to avoid detailed microphysics schemes. We compare it with several other methods. Our procedure uses the specific heat of an air parcel with water vapor and droplets included and, though small, includes specific heat and latent heat variation with temperature.

The saturation adjustment that we discuss is only a minor variation on methods that have been used, in various ways, for 60 years. The aim here is to present different saturation adjustment methods in a simple manner and to illustrate the results and impacts of our variation, which includes iteration and contributions of water vapor and liquid water mixing ratios to the specific heat of an air parcel. The impacts are relatively small but can make order 10% differences in temperature change and liquid water conversions. They could be easily implemented in any warm cloud models that uses saturation adjustment.

1. Introduction

The overall saturation adjustment situation is described by Straka (2009, Chapter 4) for cloud models. Many of the sources cited there (e.g. Rutledge and Hobbs, 1983) plus earlier models (especially Yau and Austin, 1979) present this as a time dependent adjustment.

Kogan and Martin (1994) explore results using McDonald's (1963) direct Bulk Microphysical Parameterization (BMP) approach in numerical cloud models and Langlois (1973) presented a more accurate, one-step approximate scheme for condensation of water vapor, used later by Cohard and Pinty (2000).

In our boundary layer fog and stratus cloud modelling, the dynamic/thermodynamic changes are assumed to be relatively slow (of order hours), while diffusional growth for small droplets (diameter < 5 μm), and saturation adjustments are estimated to occur in seconds and minutes if there are sufficient cloud condensation nuclei, CCN, or small droplets already present. Kogan and Martin's results (their Figure 7) suggest that their BMP scheme is reasonably satisfactory if there are more than about 50 CCN cm^{-3}. In the marine fog conditions that we are concerned with, Isaac et al (2020) generally find about 100 fog droplets per cubic centimeter.

Current weather and climate prediction models are moving to three-moment BMPs (see Liu et al, 2023), and include ice fractions as well as liquid water. Liu et al (2023) list and provide references for the BMPs used in various modules of the Weather Research and Forecasting model, WRF. These include the Thompson et al (2008), Lim and Hong (2010) and Morrison and Millbrandt (2015) schemes. All work with time stepping, and include multiple hydrometeor types. We are looking for simpler situations with our marine fog model and work on boundary-layer stratus cloud. The 1-D time dependent radiation fog model developed by Brown and Roach (1976) sets out governing equations for humidity and liquid water mixing ratios which formally include a rate of condensation term (C in their equations 1, 2 and 3). However, they make the statements "The microphysics of the condensation process is not explicitly included in the model. Instead at each time step of the integration (0.5 s) the temperature and water vapor mixing ratio are examined at every grid point. If these imply super-saturation, then condensation takes place until the air is just saturated. The appropriate latent heat adjustment is made simultaneously to the air temperature. Conversely, liquid water at a relative humidity of less than 100% is evaporated until the air is saturated or the liquid water has been used up." We have adopted the same, saturation adjustment, approach in our 1-D time dependent marine fog modelling. There have been many other relatively simple cloud and fog models, developed before and after 1976, which include BMP treatments of water vapor - fog/cloud droplet transitions in similar ways to the one we use. Using vapor pressure rather than mixing ratio, McDonald (1963) proposed essentially the same approach, as an improvement to that used by Fisher and Caplan (1963). Kessler (1995)

discusses similar schemes for convective clouds, including one described in the Kessler (1969) Meteorological Monograph. Current terminology would refer to these as one-moment BMPs. According to Straka (2009), the Soong and Ogura (1973) method is "the most popular scheme as of this (2009) writing". As with some other BMP schemes this is formulated for convective clouds and considers adjustments in a context of vertical displacement. We will show however that this is essentially the same as the initial adjustment used in our saturation adjustment, although using a different $q_s(T)$ formulation (Teten's formula).

Other schemes have been developed which include droplet numbers and are referred to as two-moment BMPs (Liu et al, 2023). Oliver et al (1978) developed a model of turbulent boundary-layer fog and low level stratus cloud along similar lines to Brown and Roach. They treat total water mixing ratio (q_t) as a dependent variable, assuming no precipitation, and split it between water vapor (q) and liquid water (ql) at the end of each model time step. They also recognise that the saturation adjustments are occurring within a turbulent flow and that departures from mean values of temperature and mixing ratios should be taken into consideration. They deal with ensemble means ($\bar{q}$,$\bar{T}$), variances ($\overline{q'^2}$) and correlations ($\overline{q'T'}$). The same issues can apply to grid volume averages in prediction models. We have not yet attempted to include these sub-grid variability effects and our saturation adjustments are simply based on local mean quantities.

Brown and Roach (1976) did not provide details of their scheme so we developed a simple code which could be useful. It is essentially a variant of the McDonald (1963) approach, but based on Bolton's (1980) empirical fit to the saturated vapor pressure, $e_s(T)$, relationship. It also uses a weighted specific heat for dry air, which is temperature dependent, mixed with water vapor and cloud droplets, and allows the latent heat (L) to vary with temperature. We iterate to improve the accuracy of the adjustment. It is described below. The essential step is to determine the temperature change during condensation or evaporation to the final equilibrium state. Mass and heat are conserved in our transitions. There is broad recognition that clouds are an important component of climate models. The method briefly described by Siebesma and Seifert (2020) as an "all or nothing" cloud parametrisarion, neglecting sub-grid variabilitty, is essentially the same as the McDonald (1963) approach and focusses on $\overline{ql}$ changes. They do however recognise the issues associated with spatial variability within a model grid volume.

2. Basic Concept and Assumptions

Consider a well-mixed volume ($q = \overline{\boldsymbol{q}}$ etc.), or air parcel, that contains dry air, water vapor (with mixing ratio q, kg/kg) and water droplets (mixing ratio, ql), and is at temperature T (K) and pressure p (Pa). The parcel density is $\rho_c = \rho_a + \rho_v + \rho_w$, and we use the term "mixing ratio" in the atmosphere specific sense, as the mass of material (water vapor or liquid water) divided by the mass of dry air. We have used the symbol q, rather than w, for these mixing ratios, as in Straka (2009). Since q and $ql << 1$ the differences with conventional chemistry and physics definitions of "mixing ratio" (mass/total mass) are small but will make differences. We also use $M = 1 + q + ql$ as the total mixing ratio of the air parcel, including dry air + water vapor + liquid water. Within an air parcel at a given temperature, T, as a result of various processes, these q and ql mixing ratios, or forecasts of their changes, may not be in thermodynamic equilibrium. The relative humidity, RH may be > 1 or we may have liquid water present with RH < 1, and changes would occur. Ignoring the many fine microphysics and chemistry details, and assuming no shortage of condensation nuclei, we assume a relatively rapid adjustment to an equilibrium situation with supersaturated air forming cloud droplets or with some cloud droplets evaporating if they are in unsaturated air. Both transformations are assumed to take place at constant total pressure (isobaric) and with no external source or sink of heat (adiabatic). The air parcel stays where it is with no vertical, or other, displacement and the saturation adjustment is assumed to be instantaneous. Temperatures will change as a result of latent heat release or requirement and we assume that dry air, water vapor and cloud droplets are all at the same temperature.

In a numerical model of cloud or fog development this saturation adjustment is made after a model time step accounting for advection and diffusion of momentum, heat, water vapor and liquid water mixing ratios, plus heating or cooling associated with radiative flux divergence. This adjustment is a major simplification of the cloud microphysics involved but for many situations a simple model can provide useful results. We use it in our modelling of boundary-layer fog and stratus cloud. As a matter of notation we will use lower case symbols, e, p, q, ql for continuous variables but upper case with numeric subscripts to specify specific values of those variables. Exceptions are T for temperature and t for time, and also M and total heat, H which will be constant in the adjustment. We suppose that, for our saturation adjustment procedure, the initial state of an air parcel is defined by T_1, Q_1, QL_1 at pressure P, and we can also compute the saturation vapor pressure $e_s(T_1)$ and saturation mixing ratio, $QS_1 = q_s(T_1, P)$. The modelled parcel may not be in microphysical equilibrium at the end of a dynamics and thermodynamics time step and for example, may have $Q_1 > QS_1$ or $Q_1 < QS_1$

and $QL_1 > 0$. The goal is to adjust the air parcel to an equilibrium state T_2, Q_2, QL_2. We assume no change in pressure and that all temperatures are > 273.15 K (0°C) to avoid complications with ice, noting that the freezing of cloud droplets and the direct deposition of ice onto ice nucleii will not always occur at 0°C and transitions may be more complex. For T > 0°C, how can we determine the new equilibrium state? Our assumptions are conservation of water mass and of heat, assuming that droplets, water vapor and dry air are well mixed and at the same temperature. Then, in this transformation process, with M as the total mass, and H, the total heat energy per unit mass of dry air (and so of M total mass), we have,

$$M = 1.0 + q + ql = \text{constant; with } q, ql \geq 0 \qquad (1)$$

and, with T in Kelvin,

$$H = qL + Mc_pT = \text{constant} \qquad (2)$$

where L is the latent heat of vaporization and c_p is a specific heat per unit total mass, at constant pressure. (Note that Cohard and Pinty (2000) use a "heat capacity" C_{ph} per unit mass of dry air so our $Mc_p = C_{ph}$).

Values for the specific heat, of dry air or water vapor, at constant pressure, and the latent heat of vaporization, include work done in expansion or compression so we do not need to consider the PV changes, where $V = 1/\rho_c$. We are just concerned with changes in sensible heat (Mc_pT) while our adjustments are at constant pressure.

Equation (2) can be simplified if we assume constant values of L and c_p in our parcel, or just use c_{pa} of dry air, at constant pressure. However, L and c_{pa} vary with T and, more significantantly, c_p should be for moist air plus liquid water. It is not always clear what other authors have done in this regard. Also, conversions from vapor pressure, e, to mixing ratio, q sometimes assume $p+e \approx p$ as in McDonald (1963). Different authors use different relationships for $e_s(T)$, $L(T)$ and $c_{pa}(T)$. Ours are given below.

The variation of L with T (K) can be approximated (Bolton, 1980) for T > 273.15K as,

$$L(T) = 2501 - 2.37(T\text{-}273.15) \quad \text{kJkg}^{-1}. \qquad (3)$$

The dry air specific heat, c_{pa} will also vary, slowly, with temperature and pressure. Tables are available and Garratt (1992) provides an equation (his Equation A20) of c_{pa} variation with temperature T(K) at standard atmospheric pressure (1013.25 hPa) as

$$c_{pa} = 1005 + (T - 250)^2/3364 \quad \text{Jkg}^{-1}\text{K}^{-1} \qquad (4)$$

For an air parcel comtaining water vapor and possibly water droplets we then have

$$c_p = (c_{pa}(T) + q\, c_{pv} + ql\, c_l)/M, \qquad \text{in J kg}^{-1}\text{ K}^{-1}. \qquad (5)$$

The specific heats c_{pv} and c_l do vary with temperature but not significantly in the range we are concernerd with (0°C to about 30°C) and we use constant values, c_{pv} = 1859.0 J kg^{-1} K^{-1} and c_l = 4217.0 J kg^{-1} K^{-1}, at 0°C from Garratt (1992). For saturation vapor pressure the Clausius-Clapeyron (CC) equation, or Tetens equation, can be used for $e_s(T)$, but, with dependence of L on T, we use the Bolton (1980) formula (Rogers and Yau, 1989, Garratt, 1992, Appendix 2), which, for T in Kelvin, is

$$e_s(T) = 611.2 \exp (17.67(T\text{-}273.15)/(T\text{-}29.65)) \qquad \text{(Pa)} \qquad (6)$$

Many such approximations are of the form $e_s(TC) = A \exp (B*TC/(TC + C))$ for temperatures, TC in °C, see Buck (1981). Bolton's formula is claimed to be within 0.1% of the best available data at that time in the range -30°C < T(C) < 35°C and the result is very close to the Clausius - Clapyron curve in the temperature range we are concerned with. For saturation water vapor mixing ratio (q_s), with the parcel under pressure, P and with the ratio of gas constants, ε = 0.622, we use

$$q_s(T) = \varepsilon\, e_s(T)/(P - e_s(T)). \qquad (7)$$

3. The saturation adjustment

As noted above the adjustment is between a non-equilibrium state (Q_1, QL_1,T_1) with $Q_1 \neq QS_1$ to an equilibrium state with $Q_2 = QS_2$, where $QS_i=QS(T_i,P)$. Note than no adjustment is needed if $Q_1 < QS_1$ and $QL_1 = 0$. It may also be possible, in cases with $Q_1 < QS_1$ and $QL_1 > 0$, to evaporate all the droplets while $Q_2 < QS_2$. Our approach would then predict $QL_2 < 0$ and adjustments are made to correct for that.

In the simple cases, but including effects of water vapour and any initial liquid water in Equation (5) for c_{p1}, and with $L_1 = L(T_1)$ we can use Equation (2) to establish that

$$H = L_1 Q_1 + Mc_{p1} T_1 = L_2 Q_2 + Mc_{p2} T_2 . \quad (8)$$

As a first approximation many adjustment schemes fit a tangent line to the $e_s(T)$ curve at T_1 and assume

$$QS_2 = QS_1 + (T_2-T_1)\, dQS/dT_1 \quad (9)$$

with dQS/dT_1 determined from differentiation of Equations (6) and (7) at T_1. If we then assume that $Q_2 = QS_2$ and, for our initial estimate (T_{2a}) of T_2, let $A = L/(Mc_p)$ be a constant, based on state 1 values, we obtain, with dQS/dT evaluated at T_1,

$$T_{2a} = T_1 + A(Q_1-QS_1)/(1 + A(dQS/dT)) . \quad (10)$$

Using Bolton's (1980) $e_s(T)$ relationship our expression for dQS/dT is

$$dQS/dT = 0.622\, P\, dES/dT / (P - ES)^2 \quad \text{where}$$

$$dES/dT = 17.67 \text{x} 243.85 \text{x} ES/(T-29.65)^2 \quad (11)$$

The corresponding Q_{2a} can be considered as either $QS(T_2)$ or as the Q_2 approximation obtained from Equation (8), but with $c_{p2} = c_{p1}$ and $L_2 = L_1$.

$$Q_{2a} = (H - Mc_{p1}T_{2a})/L_1 \quad (12)$$

Note that H can be computed from state 1 conditions, using L_1 and c_{p1}. In either case QL_{2a} is simply $M - 1.0 - Q_{2a}$ from Equation (1).

The next step is to note that $c_{p2} \neq c_{p1}$ in general and there may be a small change between L_1 and L_2. We tried various iteration schemes to improve our estimation of T_2, Q_2, QL_2. As one method, we can evaluate QS_2 at our estimated T_2a, and then use Equation (8), with $Q_2 = QS_2$, plus computed c_{p2} and L_2 values, to get another estimate of T_2.

The simplest iteration, repeatedly using $Q_2 = QS(T_2)$ in an equation derived from Equation (8), would be

$$T_2 = (H - L_2QS(T_2))/(Mc_{p2}) \quad (13a)$$

but this failed to converge. However with a relaxation factor, $\alpha = 0.75$ or 1.0, and

$$T_2 = (T_2 + \alpha(H - L_2QS(T_2))/(Mc_{p2}))/(1+\alpha) \quad (13b)$$

Equation (13b) converged satisfactorily (see Tables 1 and 2). With α = 0.5 or 2.0 there was still convergence but it was slower and we generally set α = 1.0 although convergence was faster (fewer iterations, 6 vs 9 for T changes < 10^{-4}K) with α = 0.75 in cases with RH >1.

Six sample cases are discussed in Section 6 but we can show test cases 2 and 4 in a plot of q and q_s versus T in Figure 1. Both assume an initial temperature of 288K and the initial states (Q_1 = 0,016 and 0.006) are at the top and bottom of the plot while (T_1, QS_1) is in the center. These are larger adjustments than we might expect in a single time step in a NWP or cloud model but illustrate the process well. Smaller adjustments are considered later (Table 2). The black line in the figure corresponds to the saturation mixing ratio, $QS(T)$ with Bolton's (1980) $e_s(T)$ approximation while the red dashed line is tangent to that curve at T = 288 K. Case 2 starts with (Q_1, QL_1, T_1) = (0.0160, 0, 288K). We set P = 1013.25 hPa and QS_1 can be computed as 0.0105355, so state 1 starts with about 52% supersaturation. For Case 2 the solid blue line shows $Q(T)$ decreasing as as T increases while H = constant, M = constant. The specific heat, c_p, from Equation (5) includes changing water vapor and liquid water impacts. The reduction in q would correspond to an increase in ql as T increases.

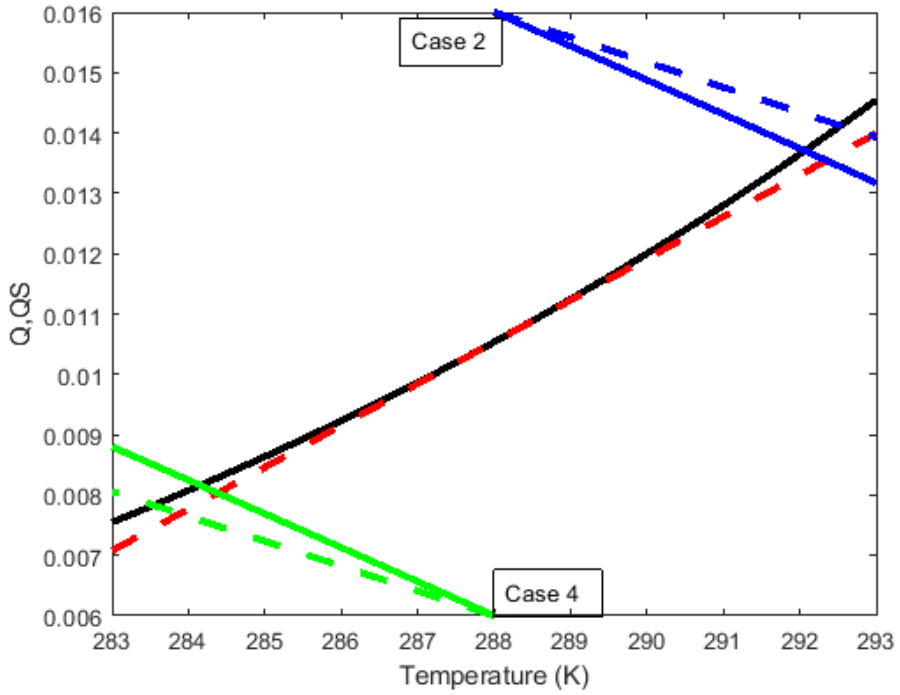

Figure 1. Two saturation adjustment cases (2 and 4 in Table 1 below) with initial temperature T_1 = 288K plus illustration of $q_s(T)$ and (dashed red line) the linear approximation $q_{sa}(T)$. The solid blue and green lines correspond to H = constant in the two cases. The corresponding dashed lines are with state 1 values of c_p and L.

Our desired saturation adjustment corresponds to the point of intersection of the solid lines, at T_2 = 292.055 K and Q_2 = 0.0136961 (Table 1). If we use the tangent *QS* line and set $c_p = c_{p1}$ in the *H* = constant line, as in our, and others, initial estimate of state 2, we get the point of intersection of the dashed lines, at T_{2a} = 292.917 K and Q_{2a} = 0.0139360. In this case the increase in temperature change relative to the correct saturation adjustment is 0.862/4.055 = 21%. The *Q* changes *(Q1-Q2a)/(Q1-Q2) = QL2a/QL2* = 0.896, so 10% less liquid water.

In Case 4 our initial state is (Q_1, QL_1, T_1) = (0.0060, 0.003, 288K). We have the same *P* = 1013.25 hPa and QS_1 can again be computed as 0.0105355 and so RH is 57%. We have set *QL* = 0.003 which provides enough liquid water to evaporate during the transition. As liquid water evaporates the temperature decreases. If there were less liquid water the saturation adjustment would predict a negative QL_2 and so checks are made to ensure that this does not occur and adjustment stops once all the liquid water has been evaporated (Case 5 in Table 1). The solid lines are with c_p from Equation (5), and would be influenced by the initial value of QL_1. The dashed lines are again with c_{p1} and the tangent to the *QS(T)* curve. Once again there is a significant difference between the points of intersection and the difference in temperature change relative to the correct value is 0.257/3.832 = 6.7%. The Q changes *(Q1-Q2a)/(Q1-Q2) = (QL1 - QL2a)/(QL1-QL2)* = 0.787, so a prediction of 20% less liquid water evaporated with no iteration.

Values are in Table 1. It is interesting that the temperature differences are greater in the supersaturated case than the evaporating droplets case but this is consistent with the relative slopes of the approximated constant H and tangent lines.

Before discussing the details of other cases we will discuss other approaches to saturation adjustment in Sections 4 and 5.

4. Other Schemes.

4.1. The Soong-Ogura adjustment scheme.

The Soong-Ogura (1973) "saturation technique" (S-O) is descibed in their appendix. It is presented in terms of potential temperature. Pressure changes are considered but, as noted by Straka (2009), Wilhelmson and Ogura (1972) argue that pressure adjustments can be ignored. For adjustments at constant pressure we can work with T in place of θ and remove π ftom the temperature adjustment equation. Soong and Ogura (1973, Equation A6) apply the same

tangential extrapolation as we have in Equations (9) and (10) and, with Teten's equation these lead to Equations (4.18) in Straka (2009) and (A9) in Soong and Ogura, (1973). Rederiving this, with our notation, T_0 = 273.15 K, a = 17.27 and c = 35.86K, and for unit mass of dry air, we obtain

$$T_2 = T_1 + B(L/Mc_p)(Q_1-QS_1) \quad \text{where} \quad B = (1+a(L/Mc_p)QS_1(T_0 - c)/(T_1-c)^2)^{-1}. \quad \text{(S4.18)}$$

Straka (2009, 4.17) has $b\Delta T$ in place of $(L/cp)QS_1$. The B expression (r_1 in Soong and Ogura. 1973) uses Teten's formula for saturation vapor pressure, which, for temperatures in K, is

$$e_s(T) = 610.78 \exp(a(T - T_0)/(T - c)) . \quad (14)$$

For saturation mixing ratio we use Equation (7), $q_s(T) = \varepsilon e_s/(p-e_s)$, where ε is the ratio of gas constants (dry air / water vapor) and is 0.622. Soong and Ogura (1973, A1) and Straka (2020, 4.7), in his presentation of the S-O scheme assume p-$e_s \approx p$ and use

$$q_s = (380/p_e) \exp(b(T - T_0)/(T - c)) \quad \text{(S4.7)}$$

where p_e (Pa) is described as "the dimensional pressure at that grid point" and c = 35.86 (Straka) or 36 (S-O). The Teten's and Bolton (1980) results for e_s are close in the temperature range we are considering, giving e_s = 1688.89 and 1687.66 Pa at 288K respectively, a less than 0.1% difference. There can however be a 1.7% difference between Equation (7), $q_s = \varepsilon e_s/(P - e_s)$ and the S-O use of $q_s = \varepsilon e_s/P$. In out S-O scheme calculations we will use Equation (7) to avoid this difference. The q_s values for p = 101325 Pa and T = 288K are then 0.0103680 and 0.0105437 without and with the p-e adjustment, while Bolton's result gives 0.0105355. Values of *T2, Q2, QL2* using the S-O scheme and Teten's equation are included in Tables 1 and 2. They are close to the first approximations with the scheme proposed here using Bolton's (1980) $e_s(T)$ approximation.

4.2 The Langlois/Cohard-Pinty adjustment scheme

Langlois (1973) presented a "rapidly convergent" approximate scheme for "large-scale condensation in a dynamical weather model". Iteration is mentioned but it is nor clear how it would be performed and it is stated that "the main conclusion to be drawn .... is that the algorithm converges rapidly. Since residuals in the parts per million range are quite

acceptable, no iteration is required for supersaturations likely to be encountered in a realistic dynarnical weather model." Cohard and Pinty (2000, Appendix C) adapted this, with some refinements, as their "non-iterative adjustment at water saturation". We will refer to it as the LCP scheme. The essential step is an extra term in the Taylor series approximation to $e_s(T)$ expanded about T_1 and a "Newton-Raphson" approximation to the solution of, with our notation,

$$F(T_2) = T_2 - T_1 + (L_1/Mc_{p1})\,(q_s(T_2) - Q_1) = 0 \qquad (15)$$

With an improved estimate of $q_s(T_2)$ they argue they argue that there is no need to iterate although we will argue that there should be iteration to account for variations in L and, more significanly, c_p values. They use a different $e_s(T)$ relationship to us but applying their analysis with the Bolton (1980) $e_s(T)$ approximation we can indeed obtain a better first estimate of T_2.

Using our notations and CP's Δs, the key equation is a variation of our Equation (10) which, with $L_1 = L(T_1)$, can be written as

$$T_2 = T_1 - \Delta_1(1 + \Delta_1\Delta_2/2) \qquad (CP1)$$

with,
$$\Delta_1 = L_1\,(QS_1 - Q_1)/(Mc_p + L_1\,DQS_1) \qquad (CP2)$$

and
$$\Delta_2 = L_1\;D2QS_1/(Mc_p + L_1\,DQS_1). \qquad (CP3)$$

where L_1 , $QS_1 = q_s(T_1)$ and derivatives $DQS_1 = dq_s/dT$ and $D2QS_1 = d^2q_s/dT^2$ are at T_1. The "heat capacity" values used by CP (Appendix D), are for unit mass of dry air, and called C_{ph}. They include water vapor and liquid water and are at (T_1, Q_1, QL_1) but not adjusted to be per unit mass of the mixture. We adjust c_p to be in $Jkg^{-1}K^{-1}$ via division by M and need to add that factor back in when dealing with mixing ratios per unit mass of dry air.

We can also note that, with $q_s = \varepsilon\, e_s/(P - e_s)$, we have.

$$dq_s/dT = \varepsilon\, P\, de_s/dT/(P - e_s)^2 \qquad (CP4)$$

and
$$d^2q_s/dT^2 = \varepsilon\, P\,(d^2e_s/dT^2/(P - e_s)^2 + 2(de_s/dT)^2/(P - e_s)^3) \qquad (CP5)$$

With the Bolton equation (4a) for $e_s(T)$ rewritten in the form

$$\ln(e_s(T)/e_{s0}) = 17.67(1 - 243.5/(T - 29.65))$$

we can differentiate to get

$$de_s/dT = 4302.645\; e_s/(T - 29.65)^2 \qquad (CP6)$$

and
$$d^2e_s/dT^2 = 4302.645\;(de_s/dT/(T - 29.65)^2 - 2e_s/(T - 29.65)^3) \qquad (CP7)$$

With no iteration the LCP non-iterative adjustment does give a better first approximation, as shown in the results in Section 6, Tables 1 and 2. However, iteration is still needed to make the $L(T)$ and c_p adjustments with (T_2, Q_2, QL_2). Curvature of $q_s(T)$ is taken into account and the temperatures, T_2, obtained from equation CP1 above approximately match the points of intersection of the curved $q_s(T)$ line and the dashed, blue and green, constant H lines which use T_1, Q_1, QL_1 values for c_p and L. In Table 2 with much smaller adjustments the LCP and simple tangent fit to the $q_s(T)$ curve give very similar results with minimal effect of curvature. Iteration to improve T_2, Q_2 and QL_2 is still needed though if more accurate saturation adjustments are required.

5. Time dependent adjustments.

Many saturation adjustment schemes proceed via a rate of change approach as described in section 4.2.1 of Straka's (2009) book. That scheme was used for example by Bryan and Fritsch (2002) who cite Rutledge and Hobbs (1983) who in turn make the statement, "Following Yau and Austin (1979) we express the (rate of) condensation of water vapor to cloud water (PCOND or dQ_v/dt in Straka's Eqn 4.4) as ...". The equation was indeed briefly presented by Yau and Austin (1979), as scheme P1, and in turn attributed to Asai (1965), who provides additional details. It is presented as a rate of change over time step Δt, sometimes using potential temperature, θ, and sometimes T. Straka's (or Yau and Austin's) equations, using our notation and T rather than θ, and with sign corrections, are,

$$dq/dt = -(q-q_s)/[(1 + L^2 q_s/Mc_pR_vT^2)\,\Delta t] \qquad \text{(S4.4)}$$

and, with M added since q is per unit mass of dry air and our c_p is per unit total mass,

$$dT/dt = -(L/Mc_p)dq/dt \qquad \text{(S4.5/6)}$$

These were modified assuming $T = \pi\,\theta$ where $\pi = (p/p_0)^{Rd/cp}$ is the Exner function. (Straka, S4.9 has an erroneous extra c_p factor). The role of Δt is rather a mystery but presumably is a measure of the time needed to reach equilibrium. I was unable to derive the S4.4 equation myself, or completely follow Asai's (1965) explanation. To some extent, and noting that Δt is undefined, this does not matter - the essential point is that as t increases, on a somewhat arbitrary scale because of Δt, $q \rightarrow q_s$. The only thing that really matters is the relative change of T with q so that H is maintained as a constant. Straka's Equation 4.5/6 should ensure this

but L and c_p will vary with T and cause complications. One approach is to assume that q has changed and then, since H is known and with the new q, we can determine T from Equ (2). This can account for L and c_p variations with T, q and ql at each time step.

We tested various approaches, using simple explicit finite differences with time step δt, in two of our test cases. We can rewrite Straka 4.4 as,

$$dq/dt = -A^*(q-q_s(T)) \text{ where } A^* = [(1 + L^2 q_s/c_p R_v T^2) \Delta t]^{-1} \quad (16a)$$

With T = 288K we hava $L^2 q_s/c_p R_v T^2 = 1.642$ and it varies from about 1.323 to 2.049 over the temperature range (284-292K) that occurs in our examples (Table 1). We left Equation (5a) in this form for comparison with other models, and took Δt = 1s. Yau and Austin (1979) appear to do that while Rutledge and Hobbs (1983) used 2 and 5s. It is never quite clear what Δt is really meant to be, but it is needed to get correct dimensions. We consider it separate from the time step used in numerical solution of Equation (16a). The basis for Asai's analysis is that predicted changes in Q without a saturation adjustment can be split between changes in Q, assuming saturation, and in QL. Yau and Austin (1979) present this as a rate of condensation and Rutledge and Hobbs (1983) and Straka (2009) note potential sensitivity to the choice of Δt, or the number of iterations.

We should emphasise that the time stepping approach works perfectly well if we simply set A^* = constant. Equation (16a) basically indicates a relaxation or adjustment of q towards q_s and the essential point is to account for T variations during this process and allow sufficient time for the adjustment to be made. A simple explicit forward stepping finite difference scheme, advancing from t to $t + \delta t$, essentially says

$$q(t +\delta t) = q(t) - A^* \delta t\, (q(t)-q_s(T)) \quad . \quad (16b)$$

An alternative, with $q_s(T)$ held fixed for that time step, is to solve Equation (16a) to give

$$q(t +\delta t) = q_s(T) + e^{-A^*\delta t}(q(t)-q_s(T)). \quad (16c)$$

which, if $A^*\delta t$ is small and $e^{-A\delta t} \approx 1 - A^*\delta t$, is the same as Equation (16b).

Instead of a finite difference representation of Equation (S4.5) we prefer to use Equation (2c), as

$$T(t + \delta t) = (H - q(t+\delta t)\, L(T(t)) /(M\, c_p(T(t))) \quad (17)$$

Ideally one would use $L(T(t + \delta t))$ and $c_p(T(t + \delta t))$, but with a slow approach to the steady state we can use L and c_p at $T(t)$ in Equation (17).

With the T = 288K cases used in Table 1, and with $A^*\delta t > 0.5$s in Equation (16a), tests showed that using the simple explicit time difference scheme, the results were unstable. However with $A^*\delta t = 0.4$s or less the forward time stepping was stable and q and T results were fully converged after 5 s with $|q - q_s| < 10^{-6}$. We generally used $A^*\delta t = 0.2$s and use 25 time steps.

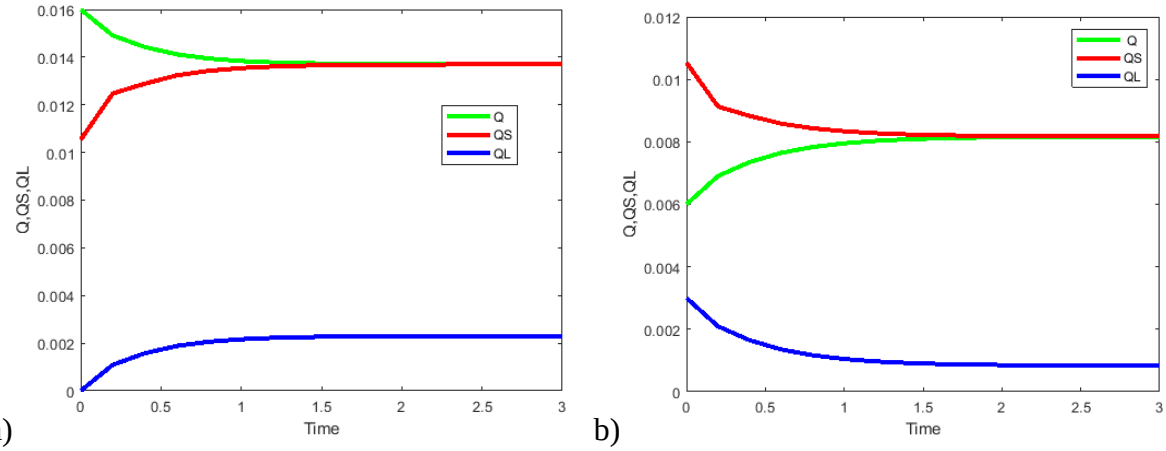

Figure 2. Time dependent adjustments for cases 2 and 4. Time is nominally in seconds but A^* or Δt are somewhat arbitrary, Here $A^*\delta t = 1$s and time step, $\delta t = 0.2$ s, so $A^* = 5.0$.

The time evolution of q, q_l and q_s with time are shown in Figure 2. In Fig 2a, water vapor from initially supersaturated air condenses, QL increases and the air warms leading to an increase in Q_S until by time ≈ 3s the air parcel is in an equilibrium state. A smoother transition is obtained with a smaller δt but the final limiting values are the same. Figure 2b illustrates a case where cloud droplets evaporate, air cools, Q_S is reduced and again things are in equilibrium by t ~ 3s. Integrations were continued until $A^*\delta t = 5$s to obtain the final values in Table 1 below. In all our cases the final near steady state exactly matched our simple iterative approach. Both are easy to apply.

6. Sample saturation adjustments: $(T_1, Q_1, QL_1) \rightarrow (T_2, Q_2, QL_2)$

6.1 Different possible situations

Our saturation adjustment can involve 4 possible situations or scenarios.

S1: Situations where $Q_1 \leq QS_1$ and $QL_1 = 0$.

We just need an initial check is to see whether any condensation or evaporation will occur.

No adjustment takes place and no changes are needed; $T_2 = T_1$; $Q_2 = Q_1$; $QL_2 = QL_1$.

S2: Situations where $Q_1 > QS_1$, $QL_1 \geq 0$.

In these circumstances where $Q_1 > QS_1$ we assume that $Q_2 = QS_2 = QS(T_2)$. the procedure is desctibed in Section 3. When applying these ideas in a dynamical model, within a model time step we are dealing with a relatively small change

S3: Situations where $Q_1 < QS_1$, $QL_1 > 0$ and $QL_2 \geq 0$

In this transition, some of the *QL* evaporates, *Q* increases, the air parcel becomes saturated and $Q_2 = QS(T_2)$, bearing in mind that as latent heat is provided for the evaporation, the air temperature and *QS* will decrease. In the equilibrium state the air parcel is saturated while some of the liquid droplets may remain. The procedure, as in **S2**, is described in Section 3. It is essential to check that $QL_2 \geq 0$ in order to maintain *M* constant. However, if all of the liquid water has evaporated before the air is saturated then those calculations lead to $QL_2 < 0$, an invalid situation needing **S4**.

S4: If $Q_1+QL_1 < QS_2$, which is not known initially, the procedure above leads to $Q_2 = QS_2$ but $QL_2 < 0$, and not acceptable. We then assume that the final equilibrium will occur with all of the liquid water evaporated and the temperature reduced by $QL_1 \, x \, L/c_p$.

Assuming conservation of heat (*H*, per unit mass of dry air) we then have an equilibrium state with

$$T_2 = (H-Q_2*L_2)/(c_{p2}*M), \quad Q_2 = Q_1 + QL_1 \quad \text{and} \quad QL_2 = 0, \tag{18}$$

Because of variation of *L* and c_{pa} with *T*, *q* and *ql*, we can again iterate to refine the T_2 estimate.

6.2 Sample Cases

In our use of this procedure in our fog/cloud model we are making adjustments after a small time increment where, at each grid point, T, Q and QL will have been modified via advection, turbulent diffusion and radiative flux divergence. The changes will be relatively small in a small time step but for illustration we can use some tests where the initial state may be somewhat different from equilibrium. Five test cases are shown in Table 1. We set T_1 = 288K and P = 101325 Pa in each case. Test 1 needs no adjustment. Tests 2 and 3 correspond to scenatio 2 above, with or without any initial *QL*. Test 4 is scenario 3 and Test 5 involves scenario 4

For cases 2 and 4 added rows indicate the first approximation values prior to iteration and calculations based on saturation adjustments proposed elsewhere. These include the Soon and Ogute (1973) scheme, Langlois (1973)/ Cohard and Pinsky(2000), or LCP, "non-iteratine adjustment" model and our time dependwent model. The widely used time dependent model often attributed to Yau and Austin (1979) and using an equation due to Asai (1965) was also used and gave identical results. These are discussed in later sections.

Table 1. Results of ADJUST test cases, T_1 = 288K, approximately 10K temperature range

Test #	T_1K	Q_1	QS_1	QL_1	T_2 K	Q_2	QS_2	QL_2	k
1 $Q_1 < QS_1$, $QL_1 = 0$	288	0.01	0.0105355	0.0	**288**	0.01	0.0105355	0.0	0
2 $Q_1 > QS_1$, $QL_1 = 0$	**288**	**0.016**	**0.0105355**	**0.0**	**292.055**	**0.0136961**	**0.0136961**	**0.0023039**	**5**
2a T_{2a}, Q_{2a}, QL_{2a}					**292.917**	0.0139360	0.0144684	0.0020640	0
2b Soong and Ogura			0.0105437		**292.963**	0.0139166	0.0145198	0.0020834	0
2c LCP estimates					**292.477**	0.0141204	0.0140698	0.0018796	0
2d Time stepping	After 5$A\delta t$, δt = 0.2s, explicit				**292.055**	0.0136961	0.0136961	0.0023039	
3 $Q_1 > QS_1$, $QL_1 > 0$	288	0.016	0.0105355	0.002	**292.042**	0.0136844	0.0136844	0.0043156	5
4 $Q_1 < QS_1$, $QL_1 > 0$	**288**	**0.006**	**0.0105355**	**0.003**	**284.168**	**0.0081681**	**0.0081681**	**0.0008319**	**8**
4a T_{2a}, Q_{2a}, QL_{2a}					**283.911**	0.0077070	0.0080278	0.0012931	0
4b Soong and Ogura			0.0105437		**283.858**	0.0077288	0.0080051	0.0012712	0
4c LCP estimates					**283.599**	0.0078369	0.0078609	0.0011631	0
4d Time stepping	After 5$A\delta t$, δt = 0.2s, explicit				**284.168**	0.0081681	0.0081681	0.0008319	
5 $Q_1 < QS_1$, $QL_1 > 0$	288	0.006	0.0105355	0.001	**286.228**	0.007000	0.0093734	0.0	5

Regarding Test 2 and Test 4 values as correct, Test 2a with no iteration overpredicts the T_2 - T_1 increase by 21% and underpredicts QL2 by 10.4%. Test 4a overpredicts the temperature decrease by 6.7% and underpredicts the QL1-QL2 decrease by 21.3%.

We see from Table 1 that total water per unit mass of dry air, (M - 1.0) and the total water, QT are always conserved, so that $Q_2+QL_2 = Q_1 + QL_1$. The total heat content per unit mass of dry air ($Q*L + c_p*T$) is also conserved with our iteration scheme (tests 2,3,4,5). The k values are the number of iterations needed to make successive T estimates agree within 10^{-4} K, but the iterative cases converge quite quickly. Relaxing the permitted "error" reduces the number of iterations, typically to 3 with 10^{-2} K temperature error tolerance. After the first step (k = 1), Q_2 is not equal to Q_{S2} but is set to $Q_S(T_2)$ in subsequent steps. Note that the iteration is

essentially to improve the estimate of T_2 but also includes changes to the values of c_p and L values as T_2 is refined. These are monitored but relatively small, of order 0.1% in L and 0.5% in c_p, in some of the tests shown. Test 1 just confirms no change if air unsaturated and no liquid water is present. In tests 2 and 3, the air starts supersaturated and temperatures rise with release of latent heat. T_1 to T_2 changes are approximately +4.06 K. With the first estimate of dQS/dT in these cases the initial difference was 4.92 K, a difference of roughly 20% of the temperature change. Tests 4 and 5 start with sub-saturated air containing liquid water. In test 4 the air parcel becomes saturated while some liquid water remains, case 2a, while in test 5 all of the liquid water has evaporated without causing saturation, case 2b. Temperature change differences are slightly smaller than in the supersaturated case but the iteration still supplies a 20% improvement. The time stepping scheme uses the Yau/Austin/Asai formulation in (corrected versions of) the equations presented by Straka (2009) and gives the same results when integrated through to a steady state. To avoid accumulation of roundoff errors at each time step we used Equation (2) to determine T after changes in Q rather than Straka's equation for $d\theta/dt$, or the time derivative of Equation (2) which would involve time detivatives $dL/dT\ dT/dt$ and dc_p/dt.

Table 2. Results of ADJUST test cases, T_1 = 288K, Q_1 = 0.99 and 1.01 times initial saturation mixing ratio, QS_1.

Test #	$T_1 K$	Q_1	Q_{S1}	QL_1	T_2 K	Q_2	Q_{S2}	QL_2	k
6 $Q_1 > QS_1$, $QL_1 = 0$	288	0.010641	0.010536	0.0	288.084	0.0105937	0.0105937	0.00004735	5
6a T_{2a}, Q_{2a}, QL_{2a}					288.095	0.0106014	0.0106015	0.00003962	0
6b Soong and Ogura			0.010544		288.089	0.0106041	0.0106053	0.00003693	0
6c LCP estimates					288.095	0.0106014	0.0106014	0.00003959	0
6d Time-stepping					288.084	0.0105936	0.0105936	0.00004735	
7 $Q_1 < QS_1$, $QL_1 > 0$	288	0.010418	0.010536	0.003	287.907	0.0104712	0.0104712	0.00294680	5
7a T_{2a}, Q_{2a}, QL_{2a}					287.894	0.0104624	0.0104628	0.00295557	0
7b Soong and Ogura			0.010544		287.886	0.0104661	0.0104650	0.00295194	0
7c LCP estimates					287.894	0.0104626	0.0104625	0.00295545	0
7d Time-stepping					287.907	0.0104712	0.0104712	0.00294680	

In our use of this procedure within a simple 1-D (z,t) time dependent fog and cloud model the adjustment procedure is called at each grid point at each time step and the changes are

smaller. In Table 2 we consider cases where State 1 is at saturation +/- 1%. Results again show that iteration still gives a substantial change in the saturation adjustments. If we compare Tests 6 and 6a we see a predicted temperature changes of 0.084K and 0.0095K so the single direct calculation is over predicted by 13% without iteration while the liquid water content is underpredicted by 16%. For Tests 7,7a the "no-iteration" changes are overprediction of delta T by 14% and underprediction of QL drop by 16%. Several factors cause these changes but the biggest effect is from changes in c_p due to contributions from the liquid water, which combine with temperature changes to give *q* and *ql* changes through Equations (2) and (1).

8. Conclusions

Many saturation adjustment schemes have been developed and used in a variety of cloud and fog models but details are sometimes hard to find. In developing our own adjustment code we decided to incorporate temperature dependence of specific and latent heats and to use a simple iterative procedure to establish an accurate equilibrium state following water vapor-cloud droplet transitions. It works satisfactorily and may be preferable to representing the adjustment as a time dependent process.

Acknowledgments.

Some initial coding was undertaken by Dr. Wensong Weng. Financial support for this research has come through a Canadian NSERC Discovery grant.

REFERENCES

Bolton, D.: The computation of equivalent potential temperature, Monthly Weather Review, 108, 1046-1053. ,1980

Brown, R. and Roach, W.T.: The physics of radiation fog: I1 - a numerical study, Quart. J. R. Met. Soc. , 102, pp. 335-354, 1976

506 Buck, A. L., 1981: New Equations for Computing Vapor Pressure and Enhancement Factor.
507 J. Appl. Meteor. Climatol., 20, 1527–1532, https://doi.org/10.1175/1520-
508 0450(1981)020<1527:NEFCVP>2.0.CO;2.

509 Cohard, J-M. and Pinty, J-P.: A comprehensive two-moment warm microphysical bulk
510 scheme. I: Description and tests, Q. J. R. Meteorol. Soc. 126, pp. 1815-1842, 2000

511 Fisher, E.L. and Caplan, P.; An experiment in numerical prediction of fog and stratus, J.
512 Atmos. Sci., 20, 425-437. 1963

513 Garratt, J.R.: The Atmospheric boundary layer, Cambridge University Press, Cambridge,
514 316pp, 1992

515 Isaac, G.A., Bullock, T., Beale, J. and Beale, S.: Characterizing and Predicting Marine Fog
516 Offshore Newfoundland and Labrador, Weather and Forecasting. 35:347-365, 2020

517 Kessler, E.: On the Distribution and Continuity of Water Substance in Atmospheric
518 Circulations. Meteorol. Monogr., 10(32), 88 pp.,1969

519 Kessler, E.: On the continuity and distribution of water substance in atmospheric circulations,
520 Atmospheric Research,38, 109-145, 1995

521 Khain, A. P., et al. (2015), Representation of microphysical processes in cloud resolving
522 models: Spectral (bin) microphysics versus bulk parameterization, Rev. Geophys., 53,
523 247–322, doi:10.1002/2014RG000468.

524 Kogan, Y.L. and Martin, W.J., Parameterization of bulk condensation in numerical cloud
525 models, J. Atmos. Sci., 51(12), 1728-1739, 1994

526 Langlois, W.E.: A rapidly convergent procedure for computing large-scale condensation in a
527 dynamical weather model, Tellus, 25:1, 86-87, DOI: 10.3402/tellusa.v25i1.963, 1973

528 Lim, K.-S. S., and S. Y. Hong,: Development of an effective double-moment cloud
529 microphysics scheme with prognostic cloud condensation nuclei (CCN) for weather and
530 climate models. Mon. Wea. Rev., 138(5), 1587−1612,
531 https://doi.org/10.1175/2009mwr2968.1. 2010

532 Liu, Y., Yau, MK., Shima, Si. et al. Parameterization and Explicit Modeling of Cloud
533 Microphysics: Approaches, Challenges, and Future Directions. Adv. Atmos. Sci. 40, 747–
534 790. https://doi-org.ezproxy.library.yorku.ca/10.1007/s00376-022-2077-3, 2023

535 McDonald, J.E.: The saturation adjustment in numerical modelling of fog, J. Atmos. Sci., 20,

476-478, 1963.

Morrison, H., and J. A. Milbrandt: Parameterization of cloud microphysics based on the prediction of bulk ice particle properties. Part I: Scheme description and idealized tests. J. Atmos. Sci., 72(1), 287−311, https://doi.org/10.1175/jas-d-14-0065.1, 2015

Oliver D. A., W. S. Lewellen and G. G. Williamson : The Interaction between Turbulent and Radiative Transport in the Development of Fog and Low-Level Stratus, J. Atmos. Sci., 35(2), 301-316, 1978

Rogers, R.R. and Yau, M.K.: A short course in cloud physics, Butterworth-Heinmann, 290pp, 1976

Rutledge, S.A. and Hobbs, P.V.: The Mesoscale and Microscale Structure and Organization of Clouds and Precipitation in Midlatitude Cyclones. VIII: A Model for the "Seeder-Feeder" Process in Warm-Frontal Rainbands, J.Atmos. Sci. 40, 1185-1206, 1983

Siebesma, A.P. and Seifert, A., 2020, Parameterising Clouds, Chapter 6 in Clouds and Climate Climate Science's Greatest Challenge, Siebsma er al, Cambtidge, 170-217.

Soong, S-T. and Ogura, Y.: A Comparison Between Axisymmetric and Slab-Symmetric Cumulus Cloud Models, J. Atmos Sci., 30, 879-893, 1973,

Straka, J.M., Cloud and Precipitation Microphysics, Cambridge University Press, 392pp, 2009

Taylor, P.A., Zheqi Chen, Li Cheng, Soudeh Afsharian, Wensong Weng, George A. Isaac1, Terry W. Bullock and Yongsheng Chen: Surface deposition of marine fog and its treatment in the WRF model, ACP discussion paper, https://acp.copernicus.org/preprints/acp-2021-344/ , 2021

Thompson, G., P. R. Field, R. M. Rasmussen, and W. D. Hall,:: Explicit forecasts of winter precipitation using an improved bulk microphysics scheme. Part II: Implementation of a new snow parameterization. Mon. Wea. Rev., 136, 5095−5115, https://doi.org/10.1175/2008MWR2387.1, 2008

Yau, M.K. and Austin, P.M.: A model for hydrometeor growth and evolution of raindrop size spectra in cumulus cells, J. Atmos Sci, 36, 655-668, 1979
